Journal of Bioenergetics and Biomembranes, Vol. 34, No. 5, October 2002 (© 2002)

Structural and Functional Insights of Wilson Disease Copper-Transporting ATPase

Negah Fatemi[1,2] and Bibudhendra Sarkar[1,2,3]

Wilson disease is an autosomal recessive disorder of copper metabolism. The gene for this disorder has been cloned and identified to encode a copper-transporting ATPase (ATP7B), a member of a large family of cation transporters, the P-type ATPases. In addition to the core elements common to all P-type ATPases, the Wilson copper-transporting ATPase has a large cytoplasmic N-terminus comprised six heavy metal associated (HMA) domains, each of which contains the copper-binding sequence motif GMT/HCXXC. Extensive studies addressing the functional, regulatory, and structural aspects of heavy metal transport by heavy metal transporters in general, have offered great insights into copper transport by Wilson copper-transporting ATPase. The findings from these studies have been used together with homology modeling of the Wilson disease copper-transporting ATPases based on the X-ray structure of the sarcoplasmic reticulum (SR) calcium-ATPase, to present a hypothetical model of the mechanism of copper transport by copper-transporting ATPases.

KEY WORDS: Wilson disease; copper-transporting ATPase; ATP7B; heavy metals; metal binding; copper-transport cycle; homology modeling; structure–function relationship; P-type ATPase; calcium-transporting ATPase.

INTRODUCTION

Wilson disease was first described in 1912 by Kinnear Wilson as a familial, lethal neurological disease accompanied by chronic liver disease leading to cirrhosis (Wilson, 1912). The disease is however, principally a disorder of hepatic copper disposition (Danks, 1995; Roberts and Cox, 1998; Sass-Kortsak, 1975; Scheinberg and Sternlieb, 1984). Copper is not incorporated into ceruloplasmin within the liver, and it is not excreted efficiently into bile. As a result, copper accumulates in the liver and is eventually released into the blood stream and deposited in other organs, notably the brain, kidneys, and cornea. This disease occurs worldwide with an average incidence of one affected individual in 30,000. The Wilson disease gene (*ATP7B*) was initially mapped to the q14.3 region of chromosome 13. Using this information as a road map, the gene abnormal in Wilson disease was identified in 1993 (Bull *et al.*, 1993; Petrukhin *et al.*, 1993; Tanzi *et al.*, 1993; Yamaguchi *et al.*, 1993). The Wilson disease gene has been shown to span at least 80 kb of genomic DNA. Sequence analysis of the cDNA indicates that it encodes a 1411 amino acid P-type ATPase (ATP7B) involved in the transport of copper. It has an extended intracellular N-terminal segment with six GMT/HCXXC copper binding motifs, eight membrane-spanning domains, three intracellular loops, and a short C-terminal. In this paper we present the current understanding and insights gained on the structural and functional aspects of Wilson disease copper-transporting ATPase.

PRODUCTION OF THE ∼72 kDa N-TERMINAL SEGMENT OF ATP7B

The N-terminal copper-binding domain (WCBD) of ATP7B contains six repeats of the heavy metal associated

[1] Department of Structural Biology and Biochemistry Research, The Hospital for Sick, Children, Toronto, Ontario, Canada.
[2] Department of Biochemistry, University of Toronto, Toronto, Ontario, Canada.
[3] To whom correspondence should be addressed at Department of Structural Biology and Biochemistry Research, The Hospital for Sick Children, 555 University Avenue, Toronto, Ontario, Canada M5G 1X8; e-mail: bsarkar@sickkids.on.ca.

0145-479X/02/1000-0339/0 © 2002 Plenum Publishing Corporation

(HMA) domain. Each domain is approximately 70 amino acids in length and contains one copy of a GMT/HCXXC motif. The precise function of this large domain in vivo remains unknown; however, the results to date imply a greater role beyond just copper binding for this domain. The production of WCBD and apo-WCBD has been previously described in detail (DiDonato et al., 1997, 2002). This procedure typically yielded protein that was >95% pure as assessed by SDS-PAGE. The refolded protein was analyzed by CD spectroscopy to confirm that the refolding procedure was successful. Addition of copper to a sample of refolded apo-WCBD resulted in Cu-WCBD with a CD spectrum that is very similar to that of soluble WCBD (Fig. 1(A)) (DiDonato *et al*., 2002), confirming that the refolding procedure had produced a natively folded WCBD capable of binding copper.

METAL-BINDING PROPERTIES

Purified WCBD was found to contain approximately six bound copper atoms (DiDonato *et al*., 1997) as determined by neutron activation analysis using GST-WCBD that was refolded in the presence of copper. This suggested that each domain is responsible for binding one copper atom. In addition to the CXXC cysteines that reside in each domain, there are six additional cysteine residues located in the regions between the metal binding domains, which may be involved in metal ligation or disulfide bridge formation.

Immobilized Metal Ion Affinity Chromatography (IMAC)

Immobilized metal ion affinity chromatography (IMAC) was used to investigate WCBD's ability to bind

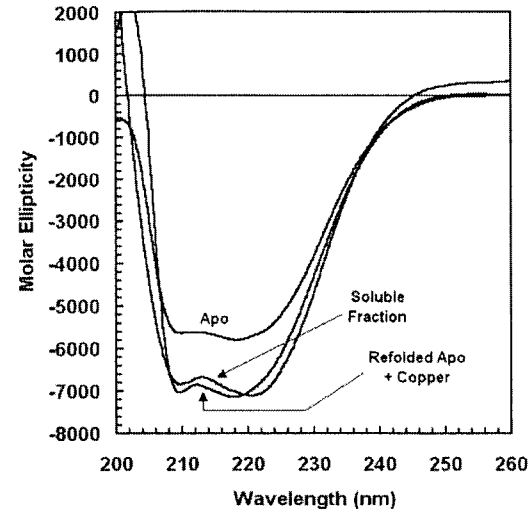

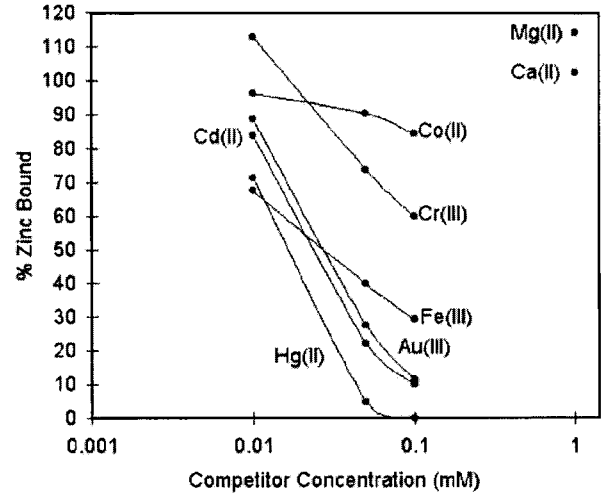

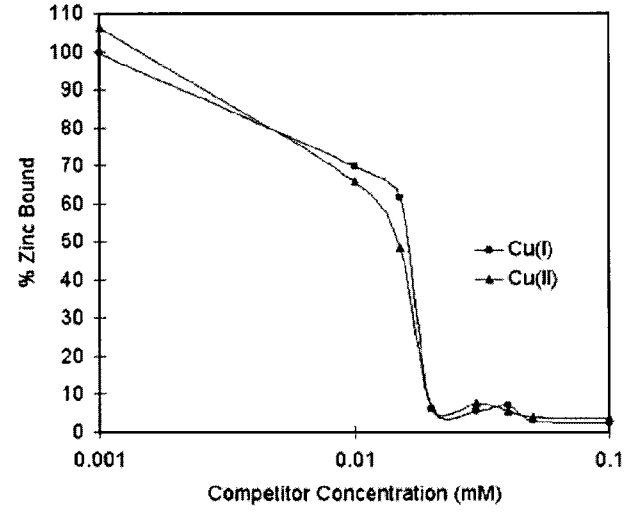

Fig. 1. (A) CD spectra of WCBD from soluble fraction, after metal removal and refolding (apo) and after addition of copper to refolded apo-WCBD (DiDonato *et al*., 2002). (B) Competition of ^{65}Zn(II) binding to WCBD with various transition metals. Samples of purified WCBD were subjected to competition ^{65}Zn(II) blotting analysis. In each case the final ^{65}Zn(II) concentration is 30 mM ($\sim\mu$10 mCi). Each competitor metal was added as the chloride salt at the indicated concentration. Successful competition resulted in a decreased signal relative to the control. Ni(II) and Mn(II) showed little or no affinity for the domain relative to Zn(II). Mg(II) and Ca(II) showed no affinity for the domain relative to Zn(II) (DiDonato *et al*., 1997). (C) Competition of ^{65}Zn(II) binding with Cu(II) (▲) and Cu(I) (●). Cu(II) was presented as the $CuCl_2$ complex while Cu(I) was presented as tetrakis(acetonitrile)copper(I) hexafluorophosphate. The Cu(I) complex was prepared in an argon-purged solution of 2% acetonitrile (DiDonato *et al*., 1997).

different metals. Samples of GST fusion protein were applied to columns charged with the indicated metal under nondenaturing, nonreducing conditions. The results were very similar regardless of whether denaturing or nondenaturing conditions were used suggesting that the major metal binding interactions are from the WCBD. The fusion protein was found to have varying affinities for columns charged with different transition metals. Based on the elution conditions, WCBD's affinity towards the different metals was as follows: Cu(II) $\gg$ Zn(II) > Ni(II) > Co(II). WCBD did not bind to columns charged with Fe(II) or Fe(III). The varying affinities may be reflective of the inability of the metal binding sites of the domain to conform to the preferred ligation geometry of certain metals. The fusion protein could only be released from the Cu(II) column using the cuprous chelator BCS. Elution of the fusion protein was accompanied by the formation of the orange ($\lambda_{max} = 480$ nm) Cu(I)BCS_2^- complex. This suggests that not only is the bound copper in the +1 oxidation state, but that Cu(II) atoms may be reduced to Cu(I) upon binding to the domain.

Competition ^{65}Zn(II)-Blotting Studies and Demonstration of Cooperativity of Copper Binding

The metal binding properties of the domain was further investigated using a ^{65}Zn(II)-blotting assay, which has previously been used to identify potential Zn(II)-binding proteins (Schiff *et al*., 1988). Preliminary experiments have shown that the domain is able to bind Zn(II) in this assay. Several metals were able to successfully compete with Zn(II) for binding to the domain. With comparison to the affinity of Zn(II) for the domain, Cd(II), Au(III), and Hg(II) seem to have the highest affinities, while Mn(II) and Ni(II) had little or no affinity (Fig. 1(B)) (DiDonato et al., 1997). Pretreatment of the membranes with DTT was critical to Zn(II) binding (data not shown), suggesting the direct involvement of free sulfhydryl groups in cysteine residues in metal chelation. Inclusion of DTT throughout the blotting experiment ensures the reduction of the disulfides. It significantly reduces the amount of nonspecific binding, most likely by chelating weakly bound metal atoms. This supports the finding that the GMT/HCXXC motif, strictly conserved in each of the metal binding domains of ATP7B as well as many bacterial heavy metal transporters is crucial for metal binding (O'Halloran, 1993; Silver *et al*., 1989). Similar results have also been reported for the metal binding properties of the MBP-fused metal domains of the Wilson and Menkes ATPases (Lutsenko *et al*., 1997).

Zn(II), Cd(II), and Hg(II) are in the same group and therefore have similar ligation geometries. The contrasting results for Fe(III) and Ni(II) obtained from IMAC and ^{65}Zn(II)-blotting experiments are probably due to the protein's inability to conform to the preferred ligation geometry of these metals while bound to the column matrix and blotting membrane respectively. The binding of metal to the domain is specific since neither Mg(II) nor Ca(II) was able to compete with Zn(II) for the binding.

Figure 1(C) (DiDonato *et al*., 1997) summarizes the results for competition blotting experiments involving copper as the competitor. At low concentrations, copper is able to decrease Zn(II) binding by about 30%; however, as the concentration increases, so does the domain's affinity for copper. This pattern was only observed for copper and may suggest that copper ligation by the domain is to some degree cooperative. The pattern is reproducible and is independent of the oxidation state of the copper indicating that the domain has similar affinities for both Cu(I) and Cu(II). The Menkes and Wilson ATPases have been localized to the trans-Golgi network (Petris *et al*., 1996; Yamaguchi *et al*., 1996) and have been shown to traffic to the plasma membrane under high copper concentrations (Forbes and Cox, 2000; Goodyer *et al*., 1999; Petris *et al*., 1996; Roelofsen *et al*., 2000; Strausak *et al*., 1999). This trafficking event could not be reproduced by adding Cd(II) or Zn(II). From these studies it has been hypothesized that the metal binding domain not only serves to ligate copper for transport but also as a copper "sensor." A similar control mechanism may be in operation for the Wilson disease protein. The domain could act as a copper sensor if the binding of multiple metal atoms was able to induce a conformational change in the domain. As the concentration of copper rises, the binding of additional metal atoms may lead to a conformational change in the domain, which may then allow the Wilson disease protein to be redistributed to another location, perhaps the canalicular membrane (Roelofsen *et al*., 2000), where it could help excrete excess copper into the bile.

STRUCTURAL STUDIES

Conformation of WCBD Upon Copper Binding

Addition of increasing amounts of copper to the WCBD resulted in a progressive increase in secondary structure as detected by CD spectroscopy (Fig. 2(A)) (DiDonato *et al*., 2000). The magnitude of this change is greatest between the apo-WCBD and the 2:1 complex and to a lesser extent from the 4:1 complex to the 6:1

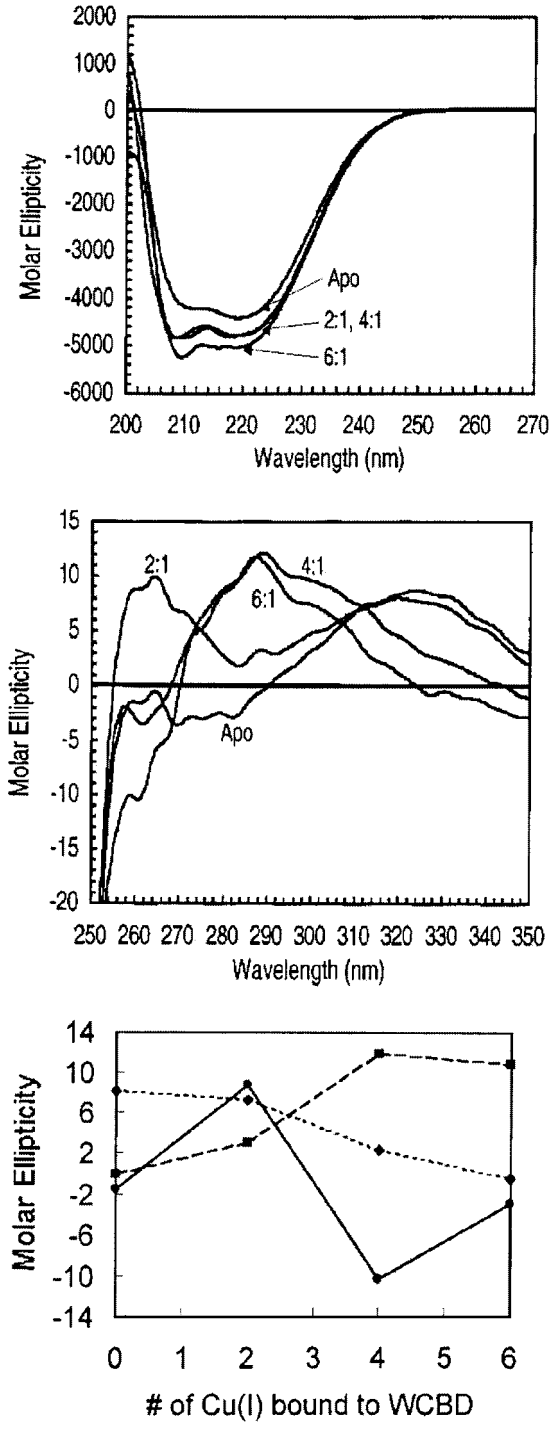

Fig. 2. Conformational changes in the WCBD induced by copper binding as monitored by CD spectroscopy (DiDonato *et al*., 2000). Samples of apo-WCBD were reconstituted with the indicated ratio of copper as determined using NAA and BCA protein assay. (A) Far UV CD spectra (secondary structure region) of Cu(I) bound WCBD. (B) Near UV CD spectra (tertiary structure region) of Cu(I) bound WCBD. (C) Molar ellipticity in the WCBD as a function of the number of Cu(I) bound per protein: molar ellipticity at 260 (●), 290 (■), and 330(♦) nm.

complex. The secondary structure changes are paralleled by drastic changes in the tertiary structure (Fig. 2(B)) (DiDonato *et al*., 2000). In the aromatic region, large changes in magnitude and line shape are observed with increasing copper content. Most interestingly, there is a progressive loss in ellipticity at ∼330 nm as more copper is bound (Fig. 2(C)) (DiDonato *et al*., 2000). Ellipticity in this region can be attributed to the presence of disulfide bonds that are present in the absence of bound copper (Wingfield and Pain, 1996). As copper is bound, the cysteine residues become involved in copper ligation and therefore are unavailable for disulfide bond formation, resulting in decrease in the ellipticity at 330 nm. It should be noted that WCBD contains six additional cysteine residues, which are not part of the GMT/HCXXC repeats. The absence of any ellipticity at 330 nm in the fully reconstituted samples suggests that these residues exist as free sulfhydryls. The 2:1 and 4:1 copper complexes are nearly identical in secondary structure, but their tertiary structure spectra are very different. It appears that the structural organization of the WCBD is being altered as each metal-binding domain becomes progressively occupied with copper. It was concluded that the tertiary structure changes could be the basis for the cooperative binding of copper, which was observed in competition ^{65}Zn(II)-blotting experiments as well (DiDonato *et al*., 1997).

XAS Studies of Copper Binding to WCBD

XAS spectra at the Cu K-edge were obtained for samples of WCBD with copper protein stoichiometries of 2:1, 3:1, and 5:1 (DiDonato *et al*., 2000). All samples exhibited a near-edge absorption (XANES) feature at 8983.5(3) eV (Fig. 3(A)) (DiDonato *et al*., 2000), consistent with the $1s \rightarrow 4p$ transition of a Cu(I) center (Kau *et al*., 1987; Pickering *et al*., 1993). For all samples studied there is a resolved peak at 8983.5(3) eV, but with an intensity that is somewhat weaker than those of digonal Cu(I) thiolate compounds but stronger than those corresponding to trigonal complexes. The intermediate nature of the XANES feature suggests that Cu(I) site in WCBD is distorted from the ideal linear geometry of a two-coordinate Cu(I) center with a S─Cu─S angle between 120° and 180°. The shape of the XANES feature appears to be independent of copper stoichiometry, indicating that all the Cu(I) sites are quite similar.

Extended X-ray absorption fine structure (EXAFS) results are consistent with the conclusions derived from XANES data above. All samples with various ratios of Cu-to-protein give rise to similar spectra, suggesting that the geometry of the Cu sites is not perturbed much with

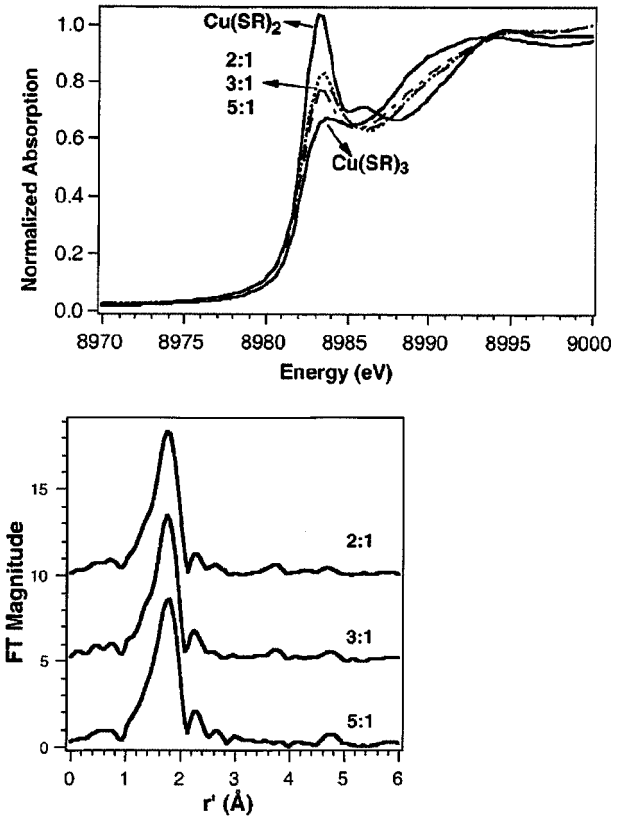

Fig. 3. XANES and EXAFS of WCBD with the indicated ratio of copper to protein (DiDonato *et al.*, 2000). (A) Normalized Cu K-Edge XANES spectra of WCBD and Cu(I)-thiolate model compounds. $Cu(SR)_2$: $[Cu(SC_{10}H_{13})_2]^-$, $Cu(SR)_3$: $[Cu(SC_6H_5)_3]_2^-$; the ratio of Cu to protein = 2:1 (dotted line), 3:1 (dashed line), and 5:1 (dotted and dashed line) (DiDonato *et al.*, 2000). (B) EXAFS of WCBD with the indicated ratio of copper to protein r'-space spectra.

different amounts of copper bound to WCBD (Fig. 3(B)) (DiDonato *et al.*, 2000). The best fit of the results consists of two S scatterers at 2.18 Å, which is most consistent with the presence of two-coordinate Cu-binding site in WCBD. Comparison of Cu—S distances of other two-coordinate Cu(I) thiolate complexes (Bowmaker *et al.*, 1984; Coucouvanis *et al.*, 1980; Dance, 1986; Fujisawa *et al.*, 1998; Koch *et al.*, 1984), strongly suggests that the Cu(I) sites in WCBD have a distorted diagonal geometry. There is no other evidence of a third scatterer in the copper coordination sphere.

A Cu—S distance of 2.16 Å has also been found in an EXAFS study of the related Menkes disease protein MNK (Ralle *et al.*, 1998) that has the same copper-binding sequence motif (GMT/HCXXC) as in WCBD. But a different copper coordination environment has been reported for Atx1, the copper chaperone protein found in yeast, which also has the same copper-binding sequence motif. Atx1 has two sulfur scatterers at 2.25 Å and a third sulfur scatterer at 2.40 Å, implicating a three-coordinate copper site (Pufahl *et al.*, 1997). Cox17, another copper chaperone protein but with a different copper-binding sequence from that of Atx1 and WCBD, also shows a Cu—S distance of 2.26 Å, indicating a three-coordinate copper-binding site (Srinivasan *et al.*, 1998). Thus there appears to be a range of possible Cu(I) binding modes for this interesting class of proteins.

SPECIFICITY OF COPPER BINDING AS DETERMINED FROM ZINC-BINDING STUDIES

Conformation of WCBD Upon Zn(II) Binding

Binding of increasing amounts of Zn(II) to WCBD gives rise to an overall loss in secondary structure content (DiDonato *et al.*, 2002). While the addition of either 2 or 4 Zn(II) atoms results in a relatively small change in the far UV CD spectra, the binding of six atoms of Zn(II) induces a sharp decrease in ellipticity. Results indicate that, although Zn(II) is able to bind to the domain fairly tightly, it seems to destabilize the domain relative to the native structure. These results are in sharp contrast to those observed for copper binding to the WCBD, which showed a progressive increase in secondary structure content as the domain binds copper. There are changes in tertiary structure also when Zn(II) binds to the WCBD. These changes are relatively small when compared to those observed for copper binding to the WCBD. The presence of positive ellipticity at 330 nm is indicative of the presence of disulfide bonds, which would be expected in the absence of metal (Wingfield and Pain, 1996). When the WCBD is titrated with copper, ellipticity at 330 nm is lost and fall to zero in the 6:1 complex as copper is bound to the cysteine residues in the domain. In contrast, when the WCBD is titrated with Zn(II), the same ellipticity at 330 nm is diminished but not completely eliminated. The presence of disulfide bonds in the 6:1 complex indicates that the bound Zn(II) atoms may not be using cysteines as their primary ligands. CD results of the Zn(II)-reconstituted WCBD support the XAS results and indicate that the ligation environment for Zn(II) is very different from that for copper.

XAS Studies of Zn(II) Binding to WCBD

Detailed structural analyses of the WCBD with various stoichiometries of Zn(II) have been carried out by XAS (DiDonato *et al.*, 2002). These studies were

performed in the presence of DTT or TCEP to determine whether the data would be affected by the addition of exogenous sulfhydryl ligands. All samples exhibited an edge energy around 9662.8 eV, which is slightly higher than that of the Zn(II) model compounds used. Not much detailed information can be obtained regarding the nature of the Zn(II) ligation, although the line shape observed is as broad as model complexes of peptides with N-scatterers (Clark-Baldwin *et al*., 1998).

The EXAFS spectra of Zn(II)–WCBD at different stoichiometries generally resemble each other. However, the major feature observed in all samples cannot be fitted with sulfur scatterers. But fitting that feature with 3–5 nitrogen scatterers at 2.03(2) Å results in significantly smaller goodness-of-fit values. Such distances are consistent with Zn(II)–imidazole ligation (Clark-Baldwin *et al*., 1998). However, a much weaker peek at $r' = 2$ Å can be modeled with a very small amount of scatterers at 2.3 Å, typical of Zn(II) thiolate bond (Clark-Baldwin *et al*., 1998). Zn(II)–sulfur scattering contribution becomes more important in the presence of higher stoichiometries of Zn(II) to WCBD. At lower Zn(II) loading, at most 1.6 sulfur per protein is involved in metal binding. This value increases to 4 in the 6:1 Zn(II)–WCBD. These results imply that Zn(II) has a higher affinity for nitrogen or oxygen ligands in the WCBD. Such ligation features are quite different from that in the Cu(I)–WCBD, where each binding site was found to ligate copper in +1 oxidation state using two cysteine side chains with a distorted two coordinate geometry (DiDonato *et al*., 2000). Although Zn(II) and copper appear to bind at different sites, it has been shown through competitive ^{65}Zn(II)-blotting experiments that Zn(II) is released when Zn(II)-reconstituted WCBD is exposed to copper (DiDonato *et al*., 1997). This suggests that the conformational changes induced by copper preclude the binding of Zn(II) and the converse is not true. Furthermore, in competition ^{65}Zn(II)-blotting experiments, the binding of Zn(II) to the WCBD could not be competed away by a 33-fold excess of either Ca(II) or Mg(II), suggesting that Zn(II) is not binding nonspecifically to the WCBD.

FUNCTIONAL STUDIES OF WCBD BY CHIMERIC PROTEINS OF ATP7B AND ZntA

There is a high degree of specificity for the metal ions that are transported by P-type ATPases. What determines this specificity is currently not known. ATP7A and ATP7B are copper-transporting ATPases. On the other hand, ZntA another P-type ATPase has been shown to be specific for Pb(II), Zn(II), Cd(II), and Hg(II) (Beard *et al*., 1997; Rensing *et al*., 1997, 1998; Sharma *et al*., 2000). To investigate the determinants of metal ion recognition and specificity for P-type ATPases, chimeric proteins were constructed in which the amino terminal domain of ZntA was replaced by the amino-terminal domain of the Wilson copper transporter ATP7B (Fig. 4) (Hou *et al*., 2001). In one chimeric protein designated WND–Cu(1–6)-ZntA, the entire amino-terminal domain of ATP7B with all six metal-binding motifs was attached to ZntA lacking its amino-terminal domain (ΔN–ZntA). In another chimeric protein, WND–Cu(6)–ZntA, only the sixth metal-binding motif of ATP7B was attached to ΔN-ZntA since it has been reported that the sixth metal-binding domain is necessary and sufficient for the transport activity of ATP7B (Forbes *et al*., 1999).

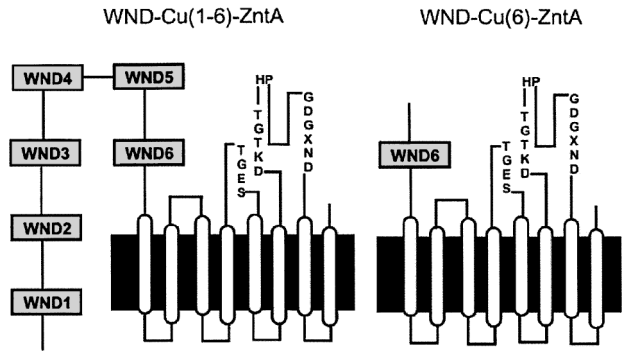

Fig. 4. Schematic representations of WND-Cu(6)-ZntA and WND-Cu(1-6)-ZntA (Hou *et al*., 2001).

Both chimeric proteins were able to confer resistance toward Pb(II), Cd(II), and Zn(II) in a ZntA-disrupted *E.coli* strain but not to copper in an *E.coli* strain disrupted in copA, which encodes a copper-transporting ATPase (Rensing *et al*., 2000). Thus it appears that the chimeras behave in a manner similar to ZntA and ΔN–ZntA but not to CopA. The purified chimeric proteins were shown to be active, the ATPase activity was stimulated by Pb(II), Cd(II), Zn(II), and Hg(II), which are substrates for ZntA. However, no activity was obtained with Cu(I) or Ag(I), cations that are substrates for ATP7B. The V_{max} values obtained for both chimeras are lower than the values obtained for ZntA, especially in the presence of thiolates in the assay buffer. The thiolate-stimulated activity is likely to be a more accurate reflection of the in vivo activity of ZntA, given that glutathione is abundant inside the cell and that metal ion chaperones present in the periplasm may assume the role of thiolates. From these results it can be concluded that metal ion specificity is determined by the transmembrane part of the ATPases. Although our studies of Zn(II) binding to WCBD suggest its involvement

in metal ion selectivity, it appears that the amino-terminal domain cannot override the intrinsic specificity of the core components of the ATPase. These results also imply that the amino-terminal domain interacts with other parts of the transporter in a metal ion specific manner. The amino-terminal domain of ATP7B cannot replace that of ZntA in restoring full catalytic activity.

It has been suggested that the full-length amino-terminal domain of ATP7B may play a regulatory role, such that metal ion binding releases an inhibitory interaction of this domain with the hydrophilic ATPase domain (Tsivkovskii *et al*., 2001a). In this case, one would expect to observe copper-stimulated ATPase activity for WND–Cu(1–6)–ZntA, but this is not observed. Therefore, at least in the case of the WND–Cu(1–6)–ZntA chimera the amino-terminal domain does not play a regulatory role (Hou *et al*., 2001).

HOMOLOGY MODELING

Knowledge about the three-dimensional (3D) structure of ATP7B is critical to our understanding of its function. However, the experimental determination of the 3D structure of this and other such proteins is not always possible due to technical challenges. Models are useful when experimental methods such as X-ray crystallography or NMR spectroscopy cannot determine the structure of a protein in time.

Homology modeling, often also called comparative protein modeling is presently the most reliable and useful 3D structure prediction method. This method takes advantage of the solved structures of closely related (homologous) proteins, to extrapolate the structure of a protein of unknown structure. One of the most important assumptions made in homology modeling is that the overall 3D structure of the target protein is similar to that of the related proteins, and that regions with sequence homology have similar structure. It is assumed that conserved residues within a family are conserved structurally, and residues involved in biological activity have similar topology throughout the protein family (Fiser and Sali, in press). Although some protein domains adopt similar folds despite no significant sequence or functional similarity, it is generally accepted that proteins from different sources with similar biological functions often have similar sequences, and that high sequence conservation is reflected by distinct structure similarity. Homology modeling can be used as a powerful tool for the structural modeling of proteins, particularly when the structures of other homologous proteins are available. In order to begin modeling the structure of a desired protein one requires, the amino acid sequence of the target protein, the high-resolution structure of at least one related protein (*template*), and any additional reference protein structures or sequences of related proteins.

The first step in homology modeling is the identification and selection of structures that will form the template for the target structure (model) (Marti-Renom *et al*., 2000). We used the 2.6 Å crystal structure of the calcium pump of sarcoplasmic reticulum, SERCA1a (Toyoshima *et al*., 2000), as the template for modeling the core P-type ATPase components of ATP7B (Fatemi and Sarkar, in press). The Na,K-ATPase (Rice *et al*., 2001), H-ATPase (Scarborough, 2000), and L-2 haloacid dehalogenase (Hisano *et al*., 1996) belong to the P-type ATPases family; these structures were used to guide the modeling of ATP7B. Each one of the six copper-binding domains in the N-terminal region of the modeled structure was based on the solution structure of the fourth metal-binding domain from the Menkes copper-transporting ATPase (Gitschier *et al*., 1998).

The 11 Å structure of the Na,K-ATPase has a high overall similarity to the E2 structure of the Ca-ATPase (Rice *et al*., 2001). Although there are several surface loops that do not align well, the cytoplasmic domains are observed to have a similar arrangement. The structural similarity between the Ca-ATPase phosphorylation domain and the catalytic domain of L-2 haloacid dehalogenase (Stokes and Green, 2000), notably the conserved positioning of important catalytic residues, suggests that the E1-to-E2 conformational change proposed for the Ca-ATPase (Toyoshima *et al*., 2000) may take place in all P-type ATPases.

The automated alignments obtained from fold assignment are generally not accurate enough, and need to be optimized by a specific sequence alignment method. Therefore, using gapped-BLAST we aligned the sequence of ATP7B representing the copper-transporting ATPases with the SERCA1a sequence (Fatemi and Sarkar, in press). For moderately similar sequences, as is the case here, the initial alignment is often rough and the boundaries of nonconserved loops are not very well defined. Therefore, the alignment was further corrected by hand in order to improve on these weaknesses. The SWISS-Model and SWISS-PDB-viewer software programs (Guex and Peitsch, 1997) were used to generate a structural alignment of homologous regions of these two transporters (Fig. 5(A)) (Fatemi and Sarkar, in press). Generally, sequences with low homology to the template protein, less than 30% sequence identity (as is the case with ATP7B and SERCA1a) are more difficult to model (Rost, 1999; Saqi *et al*., 1998) but examples of success do exist; as a rule of thumb, sequence similarity across the whole region

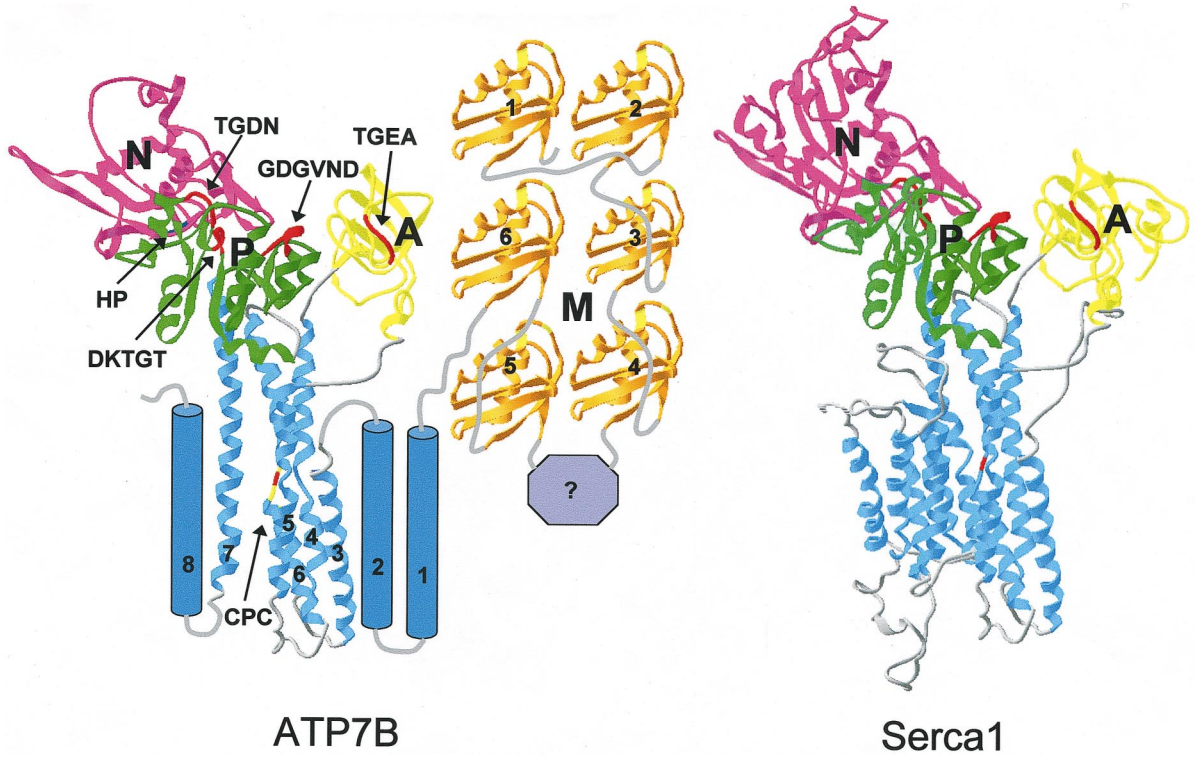
N
TGDN
GDGVND
TGEA
A
P
HP
DKTGT
M
1
2
3
4
5
6
?
8
7
5
4
3
6
2
1
CPC
N
P
A
ATP7B
Serca1

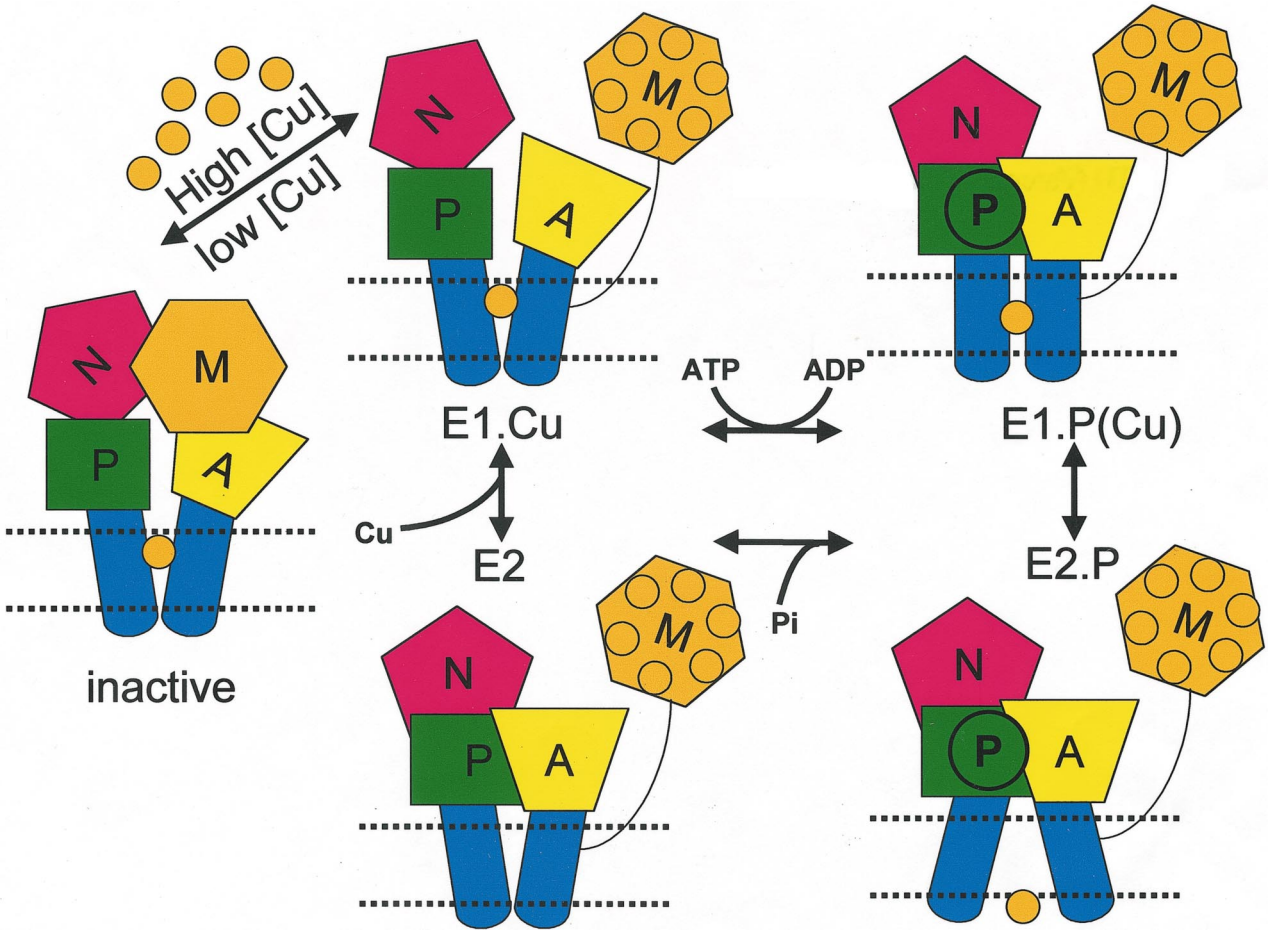
High [Cu]
low [Cu]
N
M
P
A
inactive
E1.Cu
ATP
ADP
E1.P(Cu)
Cu
E2
Pi
E2.P

is needed. Because of the low target-template sequence identity, an "align-model-realign-remodel" approach was used to optimize the model. Once the first model was computed, the alignment was inspected and improved. Secondary structure prediction and experimental findings were used in combination with mean force potential energy minimization (Sippl, 1990, 1993) to guide the model building procedure. This is a statistical method that evaluates the environment of each residue and compares it to what is expected from a representative subset of proteins. The modified alignment was then subjected to subsequent rounds of modeling and inspection, until the model could no longer be improved any further.

The multiple domains of ATP7B, were modeled separately. Insertions and deletions were incorporated into nonconserved regions where they were least likely to disrupt the overall structure. Loop regions, which cannot be modeled by homology were not modeled. Unlike the conserved regions, these loops are assumed to be flexible, and were largely disregarded in the process of modeling the conserved domains and their spatial relation to each other. The end result was a low resolution 3D model of the ATP7B structure, depicting the rough spatial organization of the various domains and conserved sequence motifs with respect to each other.

The quality of the model determines the information that can be interpreted from it, thus it is very important to be aware of the accuracy of the 3D model. A target-template sequence identity of greater than 30% often produces medium to high accuracy models. A 3D model need not be absolutely perfect or of high accuracy to be useful; but the accuracy level of the model does determine its application (Jones *et al*., 1992). Low-accuracy models display less than 30% sequence identity, and are likely to contain substantial modeling errors. However, such models can still have the correct fold and may be used to predict the approximate biochemical function of the modeled protein, or appraise the relatedness of the target and template proteins (Sanchez and Sali, 1997, 1998).

The low-resolution model of ATP7B structure generated by homology to the Ca-ATPase structure (Fig. 5(A)) (Fatemi and Sarkar, in press), implies the presence of at least four interconvertible phosphorylated and unphosphorylated conformations in the ATP-dependent copper transport cycle of Cu-ATPases. Based on what is known about the structure and mechanism of cation transport by other P-type ATPases, and based on functional studies on copper and metal-transporting P-type ATPases, the homology model of ATP7B can be used to propose a general scenario for the ATP driven transport of copper by Cu-ATPases (Fig. 5(B)) (Fatemi and Sarkar, in press).

The three cytosolic domains of P-type ATPases, the phosphorylation (P), the nucleotide-binding (N) domain, and the actuator (A) domain each play very distinct roles during ion transport. The catalytic site is comprised of the N and P domains. The copper-binding motifs found in the N-terminus (M) probably serve as the initial binding sites for the copper ions prior to transport. The N-terminal copper-binding domain has been shown to specifically bind and interact with the nucleotide-binding domain of Cu-ATPase ATP7B but not with the nucleotide-binding domain of the Na,K P-ATPase (Tsivkovskii *et al*., 2001b). In the ion-bound conformation the N and P domains form an open jaw-like formation, and therefore requiring the closure of the N and P domains to occur before phosphorylation can take place; domain closure is not dependent on the occupation of the nucleotide-binding site. Also the A domain that appears to be involved in transmission of conformational changes is largely dissociated from the main structure in the ion-bound form. This implies that cation binding in the absence of nucleotide binding weakens the interaction between the three domains. Copper binding to the N-terminus weakens its interaction with the N-domain (Tsivkovskii *et al*., 2001b) thereby causing them to dissociate. The dissociation of the N-terminus from the N-domain restores the nucleotide binding affinity of the N-domain therefore allowing the binding of ATP to the nucleotide-binding site. Nucleotide

←

Fig. 5. (A) Homology modeling of ATP7B based on the known structure of SERCA1a (Fatemi and Sarkar, in press). The core of ATP7B encompassing the regions between TM3 and TM7 can be successfully modeled. Actuator domain (A); N-terminal metal-binding domain (M); nucleotide-binding domain (N); phosphorylation domain (P). The important and conserved residues are marked on ATP7B. TM1, TM2, and TM8 do not correspond to any of the transmembrane helices in SERCA1a and were not modeled. The six copper-binding domains in the N-terminal region of ATP7B each adopt a ferredoxin-like fold found in other metal-binding domains. The region between the 4th and 5th copper-binding domains may contain a domain whose function is yet to be discovered. The overall fold of the N-terminal metal-binding domain of ATP7B is a subject of much interest and remains unknown. (B) The proposed catalytic cycle of copper transport by ATP7B (Fatemi and Sarkar, in press) based on models proposed for classical ATPases and functional studies to date is predicted to involve the following steps and intermediates. An increase in cytoplasmic copper concentration could saturate the high-affinity copper-binding sites to form E1ATP.Cu. This would activate the formation of a phosphoenzyme with ATP, occluding Cu within the protein to form the high-energy intermediate E1P.Cu. In a rate-limiting step to generate E2P, the phosphoenzyme would lose both its ability to rephosphorylate ADP and its high affinity for copper, and opens its channel to the lumen. Water then enters the catalytic site and hydrolyzes the phosphorylated aspartic acid residue to regenerate the E2 ATPase.

binding to the cation-bound state induces the association of the N- and P-domains with the A-domain, closing the gap between the domains and bringing the conserved TGEA/S motif of the A-domain close to the DKTG motif of the P-domain where phosphorylation takes place. These conformational changes are transmitted to the translocation domain, perturbing the copper-binding site within the channel, and changing its accessibility to cytosolic and lumenal spaces. In the copper-ATPases, transmembrane helices TM6, TM7, and TM8 correspond to M4, M5, and M6 of the Ca-ATPase (Toyoshima *et al*., 2000), Na,K-ATPase (Rice *et al*., 2001) and H-ATPase (Scarborough, 2000). These transmembrane domains are associated with the transduction channel and contain residues critical to cation binding. The central role of M4 has been demonstrated in a clever experiment where, the cation binding specificity of the Na,K-ATPase was altered to that of the H,K-ATPase by mutating residues within the channel (Mense *et al*., 2000). M4 and M5 are predicted to correspond to transmembrane domains TM6 and TM7 of ATP7B, respectively (Sweadner and Donnet, 2001), and both TM6 and M4 contain a conserved proline residue found in all P-type ATPases. In heavy metal-transporting ATPases, the conserved proline is flanked by a pair of cysteine residues to form the highly conserved CPC motif. Mutational analysis has shown certain residues within the copper-ATPases transmembrane domains to be critical for copper transport function, in particular the CPC motif, which is predicted to be one of the copper-binding sites within the channel (Bissig *et al*., 2001; Forbes and Cox, 1998; Voskoboinik *et al*., 2001). Mammalian copper-transporting ATPases have an additional conserved cysteine, forming a CXXCPC motif. We have constructed a peptide corresponding to residues from TM6 of ATP7B and various C/S mutants of this peptide, in our laboratory to further characterize copper binding to the CPC motif. Preliminary CD results indicate that the peptide binds a single atom of copper, and that copper binding induces secondary structure changes in the peptide (A. Myari, N. Hadjiliadis, and B. Sarkar, unpublished data). The hydrolysis of the phosphoenzyme requires the release of cation from the channel to the lumen. The release of cation may cause the movement of the A domain and allow water to access and hydrolyze the phosphoenzyme.

FUTURE DIRECTION AND CONCLUSION

Although various aspects of copper metabolism have been studied for many years, relatively little is known about the molecular mechanisms involved in the intracellular transport and excretion of copper. We have judiciously used homology modeling here as a tool in conjunction with structural and functional studies to suggest a mechanism of copper transport by copper-transporting ATPases. It is becoming increasingly evident with the advancements made in the field of structural genomics, that homology modeling will continue to play an important role in 3D structure prediction as more genomes are sequenced (Baker and Sali, 2001; Sali and Kuriyan, 1999). These studies, however, are not likely to correctly predict features that do not occur in the template, such as the structure of the N-terminal region, unique to heavy metal-transporting P-type ATPases. Further studies are needed on the mechanism and sequence of binding of copper to the N-terminal domains of the Wilson and Menkes disease proteins and how they affect their structure, and the intracellular localization and trafficking of these transporters. The identification of features within the transduction channel that confer metal ion selectivity is another exciting area to explore. These questions are only a few of the many aspects of these unique group of copper-transporting ATPases that are yet to be answered. As we gather more structural information, kinetic and functional data, it will be possible to use these in conjunction with homology modeling to construct a more detailed picture of the copper transport process through the ATPase.

ACKNOWLEDGMENTS

This research is supported by a grant from the Canadian Institutes of Health Research Grant MOP-1800.

REFERENCES

Baker, D., and Sali, A. (2001). *Science* **294,** 93–96.
Beard, S. J., Hashim, R., Membrillo-Hernandez, J., Hughes, M. N., and Poole, R. K. (1997). *Mol. Microbiol.* **25,** 883–891.
Bissig, K. D., Wunderli-Ye, H., Duda, P. W., and Solioz, M. (2001). *Biochem. J.* **357,** 217–223.
Bowmaker, G. A., Clark, G. R., Seadon, J. K., and Dance, I. G. (1984). *Polyhedron* **3**, 535–544.
Bull, P. C., Thomas, G. R., Rommens, J. M., Forbes, J. R., and Cox, D. W. (1993). *Nat. Genet.* **5,** 327–337.
Clark-Baldwin, K., Tierney, D. L., Govindaswamy, N., Gruff, E. S., Kim, C., Berg, J., Koch, S. A., and Penner-Hahn, J. E. (1998). *J. Am. Chem. Soc.* **120,** 8401–8409.
Coucouvanis, D., Murphy, C. N., and Kanodia, S. K. (1980). *Inorg. Chem.* **19,** 2993–2998.
Dance, I. G. (1986). *Polyhedron* **5**, 1037–1104.
Danks, D. M. (1995). In *Metabolic Basis of Inherited Disease* (Scriver, C. R., Beaudet, A. I., Sly, W. S., and Valle, D., eds.), McGraw-Hill, New York, pp. 2211–2235.
DiDonato, M., Hsu, H. F., Narindrasorasak, S., Que, L., Jr., and Sarkar, B. (2000). *Biochemistry* **39,** 1890–1896.
DiDonato, M., Narindrasorasak, S., Forbes, J. R., Cox, D. W., and Sarkar, B. (1997). *J. Biol. Chem.* **272,** 33279–33282.

DiDonato, M., Zhang, J., Que, L., Jr., and Sarkar, B. (2002). *J. Biol. Chem.* **31,** 31.
Fatemi, N., and Sarkar, B. (in press). *Inorg. Chim. Acta*.
Fiser, A., and Sali, A. (in press). *Methods Enzymol*.
Forbes, J. R., and Cox, D. W. (1998). *Am. J. Hum. Genet.* **63,** 1663–1674.
Forbes, J. R., and Cox, D. W. (2000). *Hum. Mol. Genet.* **9,** 1927–1935.
Forbes, J. R., Hsi, G., and Cox, D. W. (1999). *J. Biol. Chem.* **274,** 12408–12413.
Fujisawa, K., Imai, S., Kitajima, M., and Moro-oka, Y. (1998). *Inorg. Chem.* **37,** 168–169.
Gitschier, J., Moffat, B., Reilly, D., Wood, W. I., and Fairbrother, W. J. (1998). *Nat. Struct. Biol.* **5,** 47–54.
Goodyer, I. D., Jones, E. E., Monaco, A. P., and Francis, M. J. (1999). *Hum. Mol. Genet*. **8,** 1473–1478.
Guex, N., and Peitsch, M. C. (1997). *Electrophoresis* **18,** 2714–2723.
Hisano, T., Hata, Y., Fujii, T., Liu, J. Q., Kurihara, T., Esaki, N., and Soda, K. (1996). *J. Biol. Chem.* **271,** 20322–20330.
Hou, Z.-J., Narindrasorasak, S., Bhushan, B., Sarkar, B., and Mitra, B. (2001). *J. Biol. Chem.* **276,** 40858–40863.
Jones, D. T., Taylor, W. R., and Thornton, J. M. (1992). *Nature* **358,** 86–89.
Kau, L.-S., Spira-Solomon, D. J., Penner-Hahn, J. E., Hodgson, K. O., and Solomon, E. I. (1987). *J. Am. Chem. Soc.* **109,** 6433–6442.
Koch, S. A., Millar, M., and O'Sullivan, T. (1984). *Inorg. Chem.* **23,** 122–124.
Lutsenko, S., Petrukhin, K., Cooper, M. J., Gilliam, C. T., and Kaplan, J. H. (1997). *J. Biol. Chem.* **272,** 18939–18944.
Marti-Renom, M. A., Stuart, A. C., Fiser, A., Sanchez, R., Melo, F., and Sali, A. (2000). *Annu. Rev. Biophys. Biomol. Struct*. **29,** 291–325.
Mense, M., Dunbar, L. A., Blostein, R., and Caplan, M. J. (2000). *J. Biol. Chem.* **275,** 1749–1756.
O'Halloran, T. V. (1993). *Science* **261,** 715–725.
Petris, M. J., Mercer, J. F., Culvenor, J. G., Lockhart, P., Gleeson, P. A., and Camakaris, J. (1996). *EMBO J.* **15,** 6084–6095.
Petrukhin, K., Fischer, S. G., Pirastu, M., Tanzi, R. E., Chernov, I., Devoto, M., Brzustowicz, L. M., Cayanis, E., Vitale, E., Russo, J. J., Matseoane, D., Boukhgalter, B., Wasco, W., Figus, A. L., Loudianos, J., Cao, A., Sternlieb, I., Evgrafov, O., Parano, E., Pavone, L., Warburton, D., Ott, J., Penchaszadeh, G. K., Scheinberg, I. H., and Gilliam, T. C. (1993). *Nat. Genet.* **5,** 338–343.
Pickering, I. J., George, G. N., Dameron, C. T., Kurz, B., Winge, D. R., and Dance, I. G. (1993). *J. Am. Chem. Soc*. **115,** 9498–9505.
Pufahl, R. A., Singer, C. P., Peariso, K. L., Lin, S. J., Schmidt, P. J., Fahrni, C. J., Culotta, V. C., Penner-Hahn, J. E., and O'Halloran, T. V. (1997). *Science* **278,** 853–856.
Ralle, M., Cooper, M. J., Lutsenko, S., and Blackburn, N. J. (1998). *J. Am. Chem. Soc.* **120,** 13525–13526.
Rensing, C., Fan, B., Sharma, R., Mitra, B., and Rosen, B. P. (2000). *Proc. Natl. Acad. Sci. U.S.A.* **97,** 652–656.
Rensing, C., Mitra, B., and Rosen, B. P. (1997). *Proc. Natl. Acad. Sci. U.S.A*. **94,** 14326–14331.
Rensing, C., Sun, Y., Mitra, B., and Rosen, B. P. (1998). *J. Biol. Chem*. **273,** 32614–32617.
Rice, W. J., Young, H. S., Martin, D. W., Sachs, J. R., and Stokes, D. L. (2001). *Biophys. J.* **80,** 2187–2197.
Roberts, E. A., and Cox, D. W. (1998). *Baillieres Clin. Gastroenterol*. **12,** 237–256.
Roelofsen, H., Wolters, H., Van Luyn, M. J., Miura, N., Kuipers, F., and Vonk, R. J. (2000). *Gastroenterology* **119,** 782–793.
Rost, B. (1999). *Protein Eng*. **12,** 85–94.
Sali, A., and Kuriyan, J. (1999). *Trends Cell Biol*. **9,** 20–24.
Sanchez, R., and Sali, A. (1997). *Curr. Opin. Struct. Biol*. **7,** 206–214.
Sanchez, R., and Sali, A. (1998). *Proc. Natl. Acad. Sci. U.S.A.* **95,** 13597–13602.
Saqi, M. A., Russell, R. B., and Sternberg, M. J. (1998). *Protein Eng*. **11,** 627–630.
Sass-Kortsak, A. (1975). *Pediatr. Clin. North. Am.* **22,** 963–984.
Scarborough, G. A. (2000). *J. Exp. Biol*. **203**(Pt. 1), 147–154.
Scheinberg, I. H., and Sternlieb, I. (1984). *Wilson's Disease*, Saunders, Philadelphia, PA.
Schiff, L. A., Nibert, M. L., and Fields, B. N. (1988). *Proc. Natl. Acad. Sci. U.S.A.* **85,** 4195–4199.
Sharma, R., Rensing, C., Rosen, B. P., and Mitra, B. (2000). *J. Biol. Chem.* **275,** 3873–3878.
Silver, S., Nucifora, G., Chu, L., and Misra, T. K. (1989). *Trends Biochem. Sci*. **14,** 76–80.
Sippl, M. J. (1990). *J. Mol. Biol*. **213,** 859–883.
Sippl, M. J. (1993). *J. Comput-Aided Mol. Des*. **7,** 473–501.
Srinivasan, C., Posewitz, M. C., George, G. N., and Winge, D. R. (1998). *Biochemistry* **37,** 7572–7577.
Stokes, D. L., and Green, N. M. (2000). *Biophys. J*. **78,** 1765–1776.
Strausak, D., La Fontaine, S., Hill, J., Firth, S. D., Lockhart, P. J., and Mercer, J. F. (1999). *J. Biol. Chem*. **274,** 11170–11177.
Sweadner, K. J., and Donnet, C. (2001). *Biochem. J*. **356,** 685–704.
Tanzi, R. E., Petrukhin, K., Chernov, I., Pellequer, J. L., Wasco, W., Ross, B., Romano, D. M., Parano, E., Pavone, L., Brzustowicz, L. M., Devoto, M., Peppercorn, J., Bush, A. I., Sternlieb, I., Pirastu, M., Gusella, J. F., Evgrafov, O., Penchaszadeh, G. K., Honig, B., Edelman, I. S., Soares, M. B., Scheinberg, I. H., and Gilliam, T. C. (1993). *Nat. Genet*. **5,** 344–350.
Toyoshima, C., Nakasako, M., Nomura, H., and Ogawa, H. (2000). *Nature* **405,** 647–655.
Tsivkovskii, R., Eisses, J. F., Kaplan, J. H., and Lutsenko, S. (2001a). *J. Biol. Chem*. **24,** 24.
Tsivkovskii, R., MacArthur, B. C., and Lutsenko, S. (2001b). *J. Biol. Chem*. **276,** 2234–2242.
Voskoboinik, I., Greenough, M., La Fontaine, S., Mercer, J. F., and Camakaris, J. (2001). *Biochem. Biophys. Res. Commun*. **281,** 966–970.
Wilson, S. A. K. (1912). *Brain* **34,** 295–508.
Wingfield, P. T., and Pain, R. H. (1996). In *Current Protocols in Protein Science* (Coligan, J. E., Dunn, B. M., Ploegh, H. L., Speicher, D. W., and Wingfield, P. T., eds.), Wiley, New York, Vol. 1, pp. 7.6.1–7.6.23.
Yamaguchi, Y., Heiny, M. E., and Gitlin, J. D. (1993). *Biochem. Biophys. Res. Commun*. **197,** 271–277.
Yamaguchi, Y., Heiny, M. E., Suzuki, M., and Gitlin, J. D. (1996). *Proc. Natl. Acad. Sci. U.S.A*. **93,** 14030–14035.